Journal of Inflammation Research

Dovepress
Taylor & Francis Group

Open Access Full Text Article

ORIGINAL RESEARCH

A Matrigel-Free 3D Chondrocytic Spheroid Model for Rheumatoid Arthritis-Associated Synoviocytes Invasion Studies

Yingjie Zhao[1,2,*], Xuezhi Yang[3,*], Feng Yao[1,2,*], Ziwei Ouyang[2], Weirong Hu[2], Lin Li[4], Juan Cheng[5], Ke Wang[1,2], Jie Ding[2], Liang Zheng[1,2], Biao Qu[1,2], Cheng Sun[2], Shufang Li[1], Chen Jiang[2], Yanan Chen[2], Renpeng Zhou[1,2], Wei Hu[1,2]

[1]Department of Clinical Pharmacology, The Second Affiliated Hospital of Anhui Medical University, Hefei, Anhui, 230601, People's Republic of China; [2]Inflammation and Immune Mediated Diseases Laboratory of Anhui Province, Anhui Institute of Innovative Drugs, School of Pharmacy, Anhui Medical University, Hefei, Anhui, 230032, People's Republic of China; [3]Institute of Clinical Pharmacology, Anhui Medical University, Hefei, Anhui, 230032, People's Republic of China; [4]Department of Rheumatology and Immunology, The Second Affiliated Hospital of Anhui Medical University, Hefei, Anhui, 230601, People's Republic of China; [5]Department of Laboratory Medicine, The Second Affiliated Hospital of Anhui Medical University, Hefei, Anhui, 230601, People's Republic of China

*These authors contributed equally to this work

Correspondence: Renpeng Zhou; Wei Hu, Department of Clinical Pharmacology, The Second Affiliated Hospital of Anhui Medical University, Hefei, Anhui, 230601, People's Republic of China, Email zhourenpeng@ahmu.edu.cn; huwei@ahmu.edu.cn

Background: The primary pathology of rheumatoid arthritis (RA) involves the invasion of the extracellular matrix (ECM) of articular cartilage by inflammation-activated fibroblast-like synoviocytes (FLS), a process targeted by most RA therapeutic drugs. However, the absence of an efficient in vitro model for evaluating FLS invasion hinders relevant drug screening and mechanism research. To address this, a novel three-dimensional (3D) chondrocytic spheroid model that mimics cartilage ECM has been developed, along with corresponding indices to quantify synoviocytes invasion.

Methods: The matrigel-free 3D chondrocytic spheroid model was developed using an ultra-low attachment plate. The model was characterized using transcriptome sequencing, immunofluorescent staining. To explore the feasibility of this 3D chondrocytic spheroid model for evaluating the invasive capacity of synoviocytes, multi-interference strategies, including *ADAMTS5* gene overexpression, inflammatory cytokine stimulation, and anti-inflammatory drug (Etanercept) treatment were involved. Additionally, specific indices—Invasion Depth Ratio (IDR), Invasion Counts (IC), Invasion Ratio (IR), and Invasion Area Ratio (IAR)—were designed to quantify synoviocytes invasion.

Results: The 3D culture environment is more suitable for cartilage ECM synthesis by increasing cartilage anabolism-related gene (*COL2A1*) and reducing catabolism-related genes (*ADAMTS5, MMP3, CCL2 and CDKN2A*) expression. Moreover, the optimal conditions for developing the 3D chondrocytic spheroid model were identified. This model was sensitive to gene, inflammation and drug interference. Increased IDR, IC, IR and IAR was observed in *ADAMTS5* overexpressed- and IL-1β-treated chondrocytic spheroid. Further, Etanercept could inhibit TNF-α induced synoviocytes invasion of chondrocytic spheroid.

Conclusion: This matrigel-free 3D chondrocytic spheroid model offers an ideal platform for innovative drug screening and pathogenesis studies focused on synoviocytes invasion of cartilage.

Keywords: RA, invasion, 3D, synoviocytes, chondrocytes, drug screening model

Introduction

Rheumatoid arthritis (RA) is a widespread chronic inflammatory autoimmune disease, affecting approximately 0.5–1% of the global population. It is characterized by the progressive destruction of articular cartilage and subchondral bone, leading to significant disability among patients.[1,2] The invasion of articular cartilage by synovial tissue is a major driver of this destructive process. Current clinical interventions, including non-steroidal anti-inflammatory drugs, glucocorticoids, and biologic agents, primarily aim to inhibit synovial invasion to achieve therapeutic efficacy.[3] Given the growing demand for

Received: 5 November 2024
Accepted: 18 March 2025
Published: 24 March 2025

innovative drug screening and research into underlying mechanisms, there is a pressing need for the development of a new in vitro model to assess synoviocytes invasion of cartilage.

Synovial tissue plays a critical role in maintaining joint homeostasis by secreting synovial fluid, which lubricates and nourishes the avascular cartilaginous tissue. In RA, inflammatory cytokines such as tumor necrosis factor (TNF)-α and interleukin (IL)-1β trigger the abnormal activation of fibroblast-like synoviocytes (FLS) and chondrocytes. This dysregulated activation leads to the overproduction of matrix-degrading enzymes, including matrix metalloproteinases (MMPs) and a disintegrin and metalloproteinase with thrombospondin motifs (ADAMTS). These enzymes' excessive activity facilitates the invasion of synovial cells into cartilage, resulting in cartilage degradation.[4,5] Thus, targeting this pathological process represents a viable therapeutic strategy for RA treatment.

With advances in cell culture technology, three-dimensional (3D) culture systems have increasingly been shown to replicate the physiological and even pathological states of cells more effectively.[6] These systems are now widely used in preclinical screening applications.[7,8] The 3D culture system primarily comprises organoids and spheroids. Spheroids, with their simpler culturing process and shorter growth cycles, are more apt for constructing high-throughput drug screening models.[9] The main methodologies in 3D cell spheroids culture include scaffold-based systems, such as porous scaffolds[10] and matrigel scaffolds,[11] scaffold-free systems,[12] and 3D bioprinting-based systems.[13,14] Evidence suggests that 3D culture systems can closely mimic the physiological environment of cartilage, preserving chondrocytes' intrinsic phenotypes and ECM production.[15] This raises the possibility that 3D cultured cartilage models could be used instead of matrigel to assess the invasion characteristics of synoviocytes.

The matrigel-coated transwell assay is currently the standard method for assessing the invasive potential of synoviocytes. This assay quantifies invasion by counting the number of synoviocytes that penetrate the matrigel after crystal violet staining.[16] However, matrigel, originally designed to study tumor cell invasion, is composed primarily of laminin, type IV collagen (Col), entactin, and various growth factors and chemokines, closely resembling the basement membrane rather than the cartilage's extracellular matrix (ECM).[17,18] In contrast, cartilage ECM is predominantly composed of Col II and aggrecan (AGG).[19,20] As a result, Matrigel-based methods might not accurately model synoviocyte invasion into cartilage, thereby limiting research and the development of novel therapeutic strategies.

In this study, we introduced a matrigel-free 3D chondrocytic spheroid invasion model that offers several significant advantages. This model closely mimics the composition of cartilage tissue, provides controllable volume, allows for convenient drug and gene interventions, and is suitable for long-term observation with multiple evaluation parameters. Therefore, this matrigel-free 3D chondrocytic spheroid model represents an ideal platform for innovative drug screening and pathogenesis studies focused on synoviocytes invasion of cartilage.

Materials and Methods

Materials

Trypsin, penicillin/streptomycin, toluidine blue staining kit, bovine serum albumin (BSA) and 4.6-diamino-2-phenyl indole (DAPI) were procured from Beyotime Biotechnology (Shanghai, China). Fetal bovine serum (FBS), Dulbecco's Modified Eagle Medium/Nutrient Mixture F-12 (DMEM/F12) medium and GlutaMAX™-I were purchased from Gibco (Grand Island, NY, USA). PrimeSurface® 3D Cell Culture Plates were purchased from MoBiTec GmbH (Osaka, Japan). Phosphate-buffered solution (PBS) was purchased from Hyclone (South Logan, UT, USA). Puromycin was purchased from Sigma (Saint Louis, USA). Alexa Fluor® 488 Labeled Goat Anti-mouse IgG was purchased from ZSGB-BIO (Beijing, China). Matrigel was purchased from CORNING (USA). TRIzol was procured from Ambion (USA). The reverse transcription kits and TB Green premix Ex Taq were procured from TaKra BioInc., (Osaka, Japan). The recombinant human TNF-α and IL-1β were purchased from PeproTech (USA). Etanercept was procured from Guojian Pharmaceutical Co., Ltd., (Shanghai, China). The Enhanced Green Fluorescent Protein (eGFP) and ADAMTS5 overexpression lentiviral vector were constructed by Genomeditech (Shanghai, China). Anti-human Collagen II antibody was obtained from Abcam (Cambridge, UK). O.C.T. tissue embedding compound was purchased from Sakura (Osaka, Japan).

Cell Culture

The human synovial cell line (SW-982 cells) and the human cartilaginous cell line (C28/I2 cells) were sourced from Pricella Biotechnology Co., Ltd. in Wuhan, China. These cells were cultured under standard conditions, being maintained in DMEM/F12 medium supplied with 10% FBS, 1% penicillin-streptomycin, and 1× GlutaMAX™-I. The culture environment was set to 37°C with a 5% CO_2 atmosphere to ensure optimal growth and proliferation.

Quantitative Real-Time PCR

Total RNA was extracted from 2D/3D-cultured C28/I2 cells using TRIzol and quantified spectrophotometrically at 260 nm, with purity assessed by the 260/280 nm ratio. RNA was reverse transcribed into cDNA, which was then subjected to qPCR under the following conditions: 95°C for 10 min, 40 cycles of 95°C for 5s and 61°C for 10s, followed by a melt curve analysis from 65 to 95°C. *GAPDH* served as an internal control, and relative mRNA expression was calculated using the $^{\Delta\Delta}$Ct method, with fluorescence signals collected during the extension phase and Ct values recorded for analysis. The fluorescence signal was collected in the extended period, the Ct value of the sample was recorded using $2^{-\Delta\Delta Ct}$ method. The relative primer sequences were listed in Supplementary Table 1.

Transcriptome Sequencing (RNA-Seq)

RNA-seq data were generated for both 2D and 3D culture groups, with three biological replicates conducted to assess global gene expression changes. The quality of the total RNA was evaluated using an ND-1000 Nanodrop spectrophotometer and an Agilent 2200 Tape Station, ensuring that the A260/A280 ratio exceeded 1.8, the A260/A230 ratio was greater than 2.0, and the RNA integrity number was above 7.0. RNA-seq libraries were constructed with the TruSeq RNA Sample Preparation Kit from Illumina, and sequencing was performed on an Illumina HiSeq 2500 system for high-throughput analysis. Differentially expressed genes (DEGs) were identified with a fold change cutoff of greater than 2 and a *P*-value less than 0.05. These DEGs were further analyzed in relation to growth and biochemical indices to elucidate the genetic differences between the 2D and 3D culture conditions.

Cell Transfection

The *ADAMTS5* and *eGFP* overexpression lentivirus with puromycin resistance gene was produced by Genomeditech (Shanghai, China). To facilitate transfection, C28/I2 or SW-982 cells were exposed to the lentiviral vector for a period of 12 h. post-transfection, the cells were subjected to selection using 1 μg/mL of puromycin for 5 days, and were subsequently maintained in the presence of 500 ng/mL of puromycin, as per the manufacturer's guidelines for the lentivirus. The infection efficiency was confirmed by fluorescence microscope.

3D Chondrocytic Spheroid Culture, Evaluation and Coculture With Synoviocytes

Larger chondrocytic spheroids are advantageous for invasion experiments due to their improved observability. To determine the optimal conditions for constructing 3D chondrocytic spheroids, various cell quantities and time intervals were tested. In brief, PrimeSurface® 3D Cell Culture Plates were first moistened with serum-free DMEM/F12 medium. Then, varying densities of C28/I2 cells (5×10^3, 1×10^4, 2×10^4, 3×10^4, 4×10^4/150 μL) were seeded into individual wells. The internal structure of the 3D chondrocytic spheroids was scanned by high-content Z-axis (Supplementary Materials 1). The chondrocytic spheroids were collected on Day 4 (D4). To pinpoint the ideal culture duration, 3×10^4 C28/I2 cells were seeded in each well, and incubated for a period ranging from 1 to 5 days prior to harvesting. The medium was half-refreshed every second day, with careful attention to avoid disturbing the chondrocytic spheroids at the bottom of the wells during the media change. The diameter of the chondrocytic spheroids was measured using Image J software, allowing for a quantitative analysis of spheroid size to inform the establishment of the most favorable conditions for spheroid formation. To compare the sphere diameters and evaluate the advantages of the matrigel-free 3D chondrocytic spheroids, we also constructed chondrocytic spheroids using the traditional matrigel-based method, as described in Supplementary Materials 1.

In the coculture assay, the previously established chondrocytic spheroids were carefully relocated to fresh wells using sterile Pasteur pipettes. Subsequently, 6×10^3 eGFP-overexpressing SW-982 synoviocytes (pretreated with 25 ng/mL TNF-α for 24 h) in 50 μL medium were seeded upon the spheroids. The synoviocytes and chondrocytic spheroids

were then cocultured for an additional 48 h before further analysis. To investigate the invasion process, the spheroids were initially fixed using 4% paraformaldehyde and subsequently stained with DAPI for 20 min to visualize the nuclei. Representative images were captured at three distinct time points: 0 h, 6 h, and 24 h post-seeding of the synoviocytes.

To assess the suitability of this in-vitro 3D chondrocytic spheroids model for future screening of therapeutic targets and drugs related to the process of synovial-cartilage invasion, we implemented three intervention strategies. Prior to the coculture process, we (1) manipulated the chondrocytic spheroids model by altering gene expressions (*ADAMTS5* gene were overexpressed in C28/I2 cells before 3D culture), modulating inflammatory cytokine levels (chondrocytic spheroids were pretreated with 20 ng/mL IL-1β for 24 h before coculturing), and introducing specific drugs (SW-982 synoviocytes were pretreated with 25 ng/mL of TNF-α, either alone or in combination with 200 ng/mL of the TNF-α inhibitor Etanercept for 24 h before coculturing).[21] These experimental modifications were designed to explore the potential effects of these variables on synovial invasion, thereby validating the utility of this model in screening for disease-modifying interventions.

Frozen Section and Observation

The 3D chondrocytic spheroids, either constructed or cocultured, were first rinsed with PBS to remove residual media and then collected in 500 μL centrifuge tubes. Following this, the spheroids were stained with toluidine blue for 2 min, a procedure that facilitates their identification during subsequent analysis. The staining was followed by a 10-min fixation in 4% paraformaldehyde to stabilize the cellular structures. After fixation, the stained spheroids underwent dehydration through sequential immersion in 15% and 30% sucrose solutions, each for 48 h at 4°C, until they sank to the bottom of the tubes. Finally, OTC was employed to embed the spheroids, allowing for the preparation of 5 μm thick frozen sections. These sections were then ready for further microscopic examination and analysis.

To assess the expression levels of type II collagen in 3D chondrocytic spheroids, the sections were first washed with PBS and then treated with EDTA antigen retrieval solution for 10 min. Following this, the sections underwent three successive PBS washes, 5 min each. They were then blocked with 0.5% BSA for 1 h to prevent non-specific binding. Subsequently, sections were incubated with anti-collagen II antibody (1:200) overnight at 4°C. On the following day, the sections were incubated with Alexa Fluor 488-conjugated secondary antibodies at room temperature for 1 h, followed by three additional PBS washes, 3 min each. The sections were then stained with DAPI for 10 min to highlight the nuclei, after which they were treated with an anti-fluorescence quenching agent. Finally, images were captured by a fluorescence microscope (ZEISS, Germany).

To assess the degree of synoviocytes invasion, the sections were stained with DAPI for 10 min and then sealed with an anti-fluorescent quencher. The sections were then examined under a fluorescence microscope to identify and quantify the invasive synoviocytes. Three specific indices were used to measure the invasion degree: the Invasion Depth Ratio (IDR), the Invasion Counts (IC) and the Invasion Area Ratio (IAR).

The IDR was calculated using the formula:

$$\text{Invasion Depth Ratio}(IDR) = \frac{c}{(a+b)/2} \times 100\%$$

where c represents the distance from the invasive synoviocytes to the center of the spheroid, and a and b are the long and short radius of the spheroid, respectively. The a, b and c were measured by ImageJ software.

The IC was calculated using the formula:

$$\text{Invasion Counts}\,(IC) = invasivecells$$

The IAR was calculated using the formula:

$$\text{Invasion Area Ratio}\,(IAR) = \frac{a'}{a} \times 100\%$$

where a′ represents the area of invaded SW-982 synoviocytes within the spheroids, as measured by ImageJ software, while a denotes the total sectional area of the chondrocytic spheroids.

Flow Cytometry

After coculturing the chondrocytic spheroids with SW-982 synoviocytes, they were washed with PBS to remove any synoviocytes that had not infiltrated the spheroids. Subsequently, the spheroids were digested with 100 μL of trypsin for 2 min to dissociate the cells. This digestion was halted by the addition of 100 μL of complete medium. The resulting cell suspension was then subjected to analysis by flow cytometry. The specific index, Invasion Ratio (IR) was designed to evaluate the invasion degree.

The IR was calculated using the formula:

$$\text{Invasion Ratio } (IR) = \frac{n'}{n}$$

where n' represents the count of SW-982 synoviocytes inside the spheroids as measured by flow cytometry, and n is the initial number of SW-982 synoviocytes added to the coculture.

Statistical Analysis

The data were analyzed using GraphPad Prism (GraphPad Software, La Jolla, USA). All experiments were conducted with a minimum of three independent biological replicates and results are displayed as means ± standard error of mean (SEM). Statistical differences between groups were determined using either a *t*-test or one-way analysis of variance (ANOVA). A *p*-value of less than 0.05 was considered to indicate statistical significance.

Results

Comparison of Gene Expression Profiles Between 2D and 3D Culture of C28/I2 Chondrocytes

Expression Changes of Genes and Enrichment Analysis of Pathways in 2D and 3D Cultures

Transcriptome analysis was conducted to investigate the alterations in gene expression and pathway enrichment related to anabolism, catabolism, inflammation, and apoptosis between 2D and 3D-cultured C28/I2 chondrocytes (Figure 1A). Using DEseq2 for statistical analysis, DEGs were identified based on a fold change (|log2 (fold change)| > 1) and significance level (P < 0.05). A total of 1502 DEGs were identified, with 649 up-regulated and 853 down-regulated (Supplementary Figure 1A). Comparative enrichment analysis of the differentially expressed genes, including Gene Ontology (GO) Term (Figure 1B), Kyoto Encyclopedia of Genes and Genomes (KEGG) (Figure 1C), and GO enrichment (Supplementary Figure 1B), revealed that pathways related to inflammatory response, extracellular matrix degradation, apoptosis, cell senescence, and metallopeptidase activity were downregulated in 3D-cultured C28/I2 chondrocytes. A heat map of the differentially expressed genes indicated that genes associated with cartilage ECM anabolism were expressed at higher levels under 3D culture conditions, whereas genes related to cartilage ECM catabolism, inflammation, and apoptosis were relatively downregulated (Figure 1D). Similarly, GSEA analysis highlighted significant differences in gene expression signatures related to metallopeptidase activity (Figure 1E) and inflammatory response (Figure 1F) between the groups. These findings suggest that C28/I2 chondrocytes are better able to maintain their favorable state in a 3D culture system.

Expression of Anabolism and Catabolism Related Genes in 2D- and 3D-Cultured Chondrocytes

PCR was further employed to verify changes in anabolic and catabolic gene expression in C28/I2 chondrocytes cultured in both 3D and 2D systems. The results revealed that, compared to 2D culture, the expression of *COL2A1*, which is related to cartilage ECM synthesis, was significantly upregulated in 3D cultured C28/I2 chondrocytes (Figure 2A). Conversely, the expression of genes associated with abnormal fibrotic cartilage differentiation (*COL1A1, COL5A1, COL11A1*) was significantly reduced (Figure 2B–D). Additionally, genes linked to cartilage catabolism (*ADAMTS5, MMP3*), inflammatory chemokine (*CCL2*), and senescence markers (*CDKN2A*) were also significantly diminished in 3D cultured C28/I2 chondrocytes (Figure 2E–H). These findings suggest that 3D culture conditions are more favorable for preserving chondrocyte stability and better replicate the cartilage ECM environment.

https://doi.org/10.2147/JIR.S504701

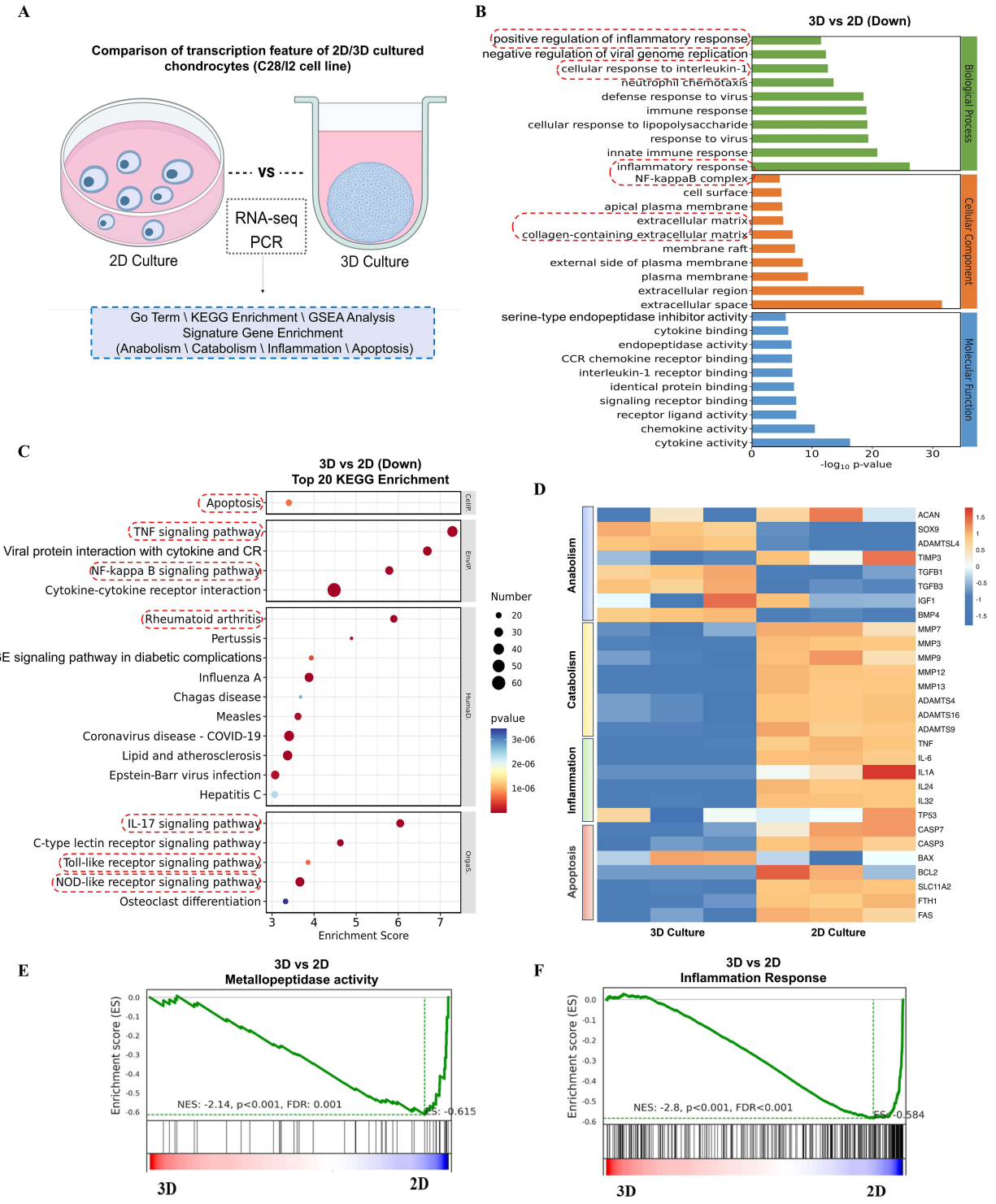

Figure 1 Comparison of gene expression profiles between 2D and 3D culture of C28/I2 chondrocytes. (**A**) Experimental Schematic: RNA-seq and PCR assays were employed to compare the variation of genes and pathways between 2D- and 3D-cultured C28/I2 chondrocytes. (**B**) GO term analysis was conducted to examine the functional enrichment of differential genes involved in the biological processes of 2D- and 3D-cultured chondrocytes (n = 3). The red dashed boxes show enriched biological processes related to cartilage matrix catabolism. (**C**) KEGG enrichment analysis was performed to investigate the enrichment o C28/I2f differential genes in signaling pathways between 2D- and 3D-cultured C28/I2 chondrocytes (ordered by p value) (n = 3). The color and size of the dots represent the range of p-values and the number of DEGs for the indicated pathway, respectively. The red dashed boxes show enriched signaling pathways related to cartilage matrix catabolism. (**D**) Heat maps of DEGs illustrated the changes in anabolic, catabolic, inflammatory, and apoptosis-related genes in 2D- and 3D-cultured C28/I2 chondrocytes (n = 3). (**E**) GSEA showing metallopeptidase activity in 2D- and 3D-cultured C28/I2 chondrocytes (n = 3). (**F**) GSEA showing inflammation response in 2D- and 3D-cultured C28/I2 chondrocytes (n = 3).

https://doi.org/10.2147/JIR.S504701

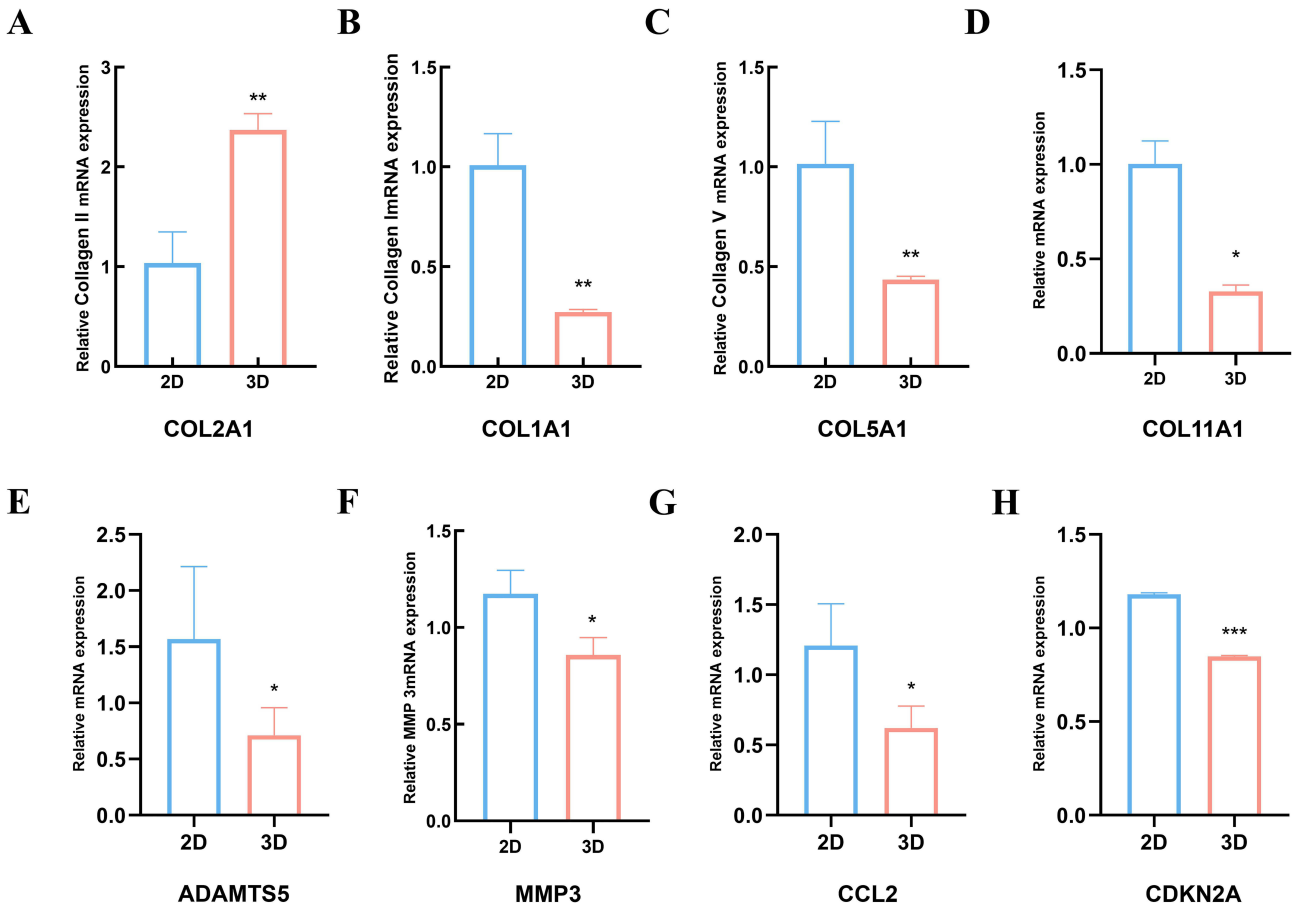

Figure 2 Expression of anabolism and catabolism related genes in 2D- and 3D-cultured chondrocytes. PCR assays were conducted to measure the expression of (**A**) *COL2A1*, (**B**) *COL1A1*, (**C**) *COL5A1*, (**D**) *COL11A1*, (**E**) *ADAMTS5*, (**F**) *MMP3*, (**G**) *CCL2*, and (**H**) *CDKN2A* genes in 2D- and 3D- cultured chondrocytes (n = 3). **P*<0.05, ***P*<0.01, ****P*<0.001 *versus* 2D.

Construction of 3D Culture of Chondrocytes

The diameter of a chondrocytic spheroids plays a crucial role in facilitating the observation of synoviocytes invasion. In this study, we compared chondrocytic spheroids generated via the traditional matrigel-based method with those produced using a matrigel-free approach. Our findings revealed that the average diameter of chondrocytic spheroids formed by the traditional method was less than 100 μm, which is considerably smaller than the approximately 500 μm average diameter observed in spheres created by the matrigel-free technique utilized in this experiment (Supplementary Figure 2A and B). These results indicate that chondrocytic spheroids established by the matrigel-free method are more suitable for studying synoviocytes invasion.

To evaluate the impact of the number of inoculated cells on the formation of 3D chondrocytic spheroids, we conducted spheroids formation experiments using varying cell quantities (Figure 3A). The results indicated that the diameter of the chondrocytic spheroids increased proportionally with the number of cells (Figure 3B). However, when the cell count reached 40,000 cells/well, the chondrocytic spheroids exhibited a hollow structure, a finding corroborated by high-content Z-stacks scanning (Supplementary Figure 3). These observations suggest that 30,000 cells/well is the optimal cell quantity for constructing chondrocytic spheroids, balancing both the maximum sphere diameter and structural integrity.

To investigate the impact of varying culture durations on the formation of 3D chondrocytic spheroids, we designed a series of observations at different time points (Figure 3C). The results demonstrated that the diameter of the chondrocytic spheroids gradually decreased as the culture time increased (Figure 3D). By the fourth day, the average diameter of the chondrocytic spheroids had stabilized, indicating that the fourth day is the optimal time point for the establishment of chondrocytic spheroids. Additionally, immunofluorescence was employed to observe the expression of

https://doi.org/10.2147/JIR.S504701

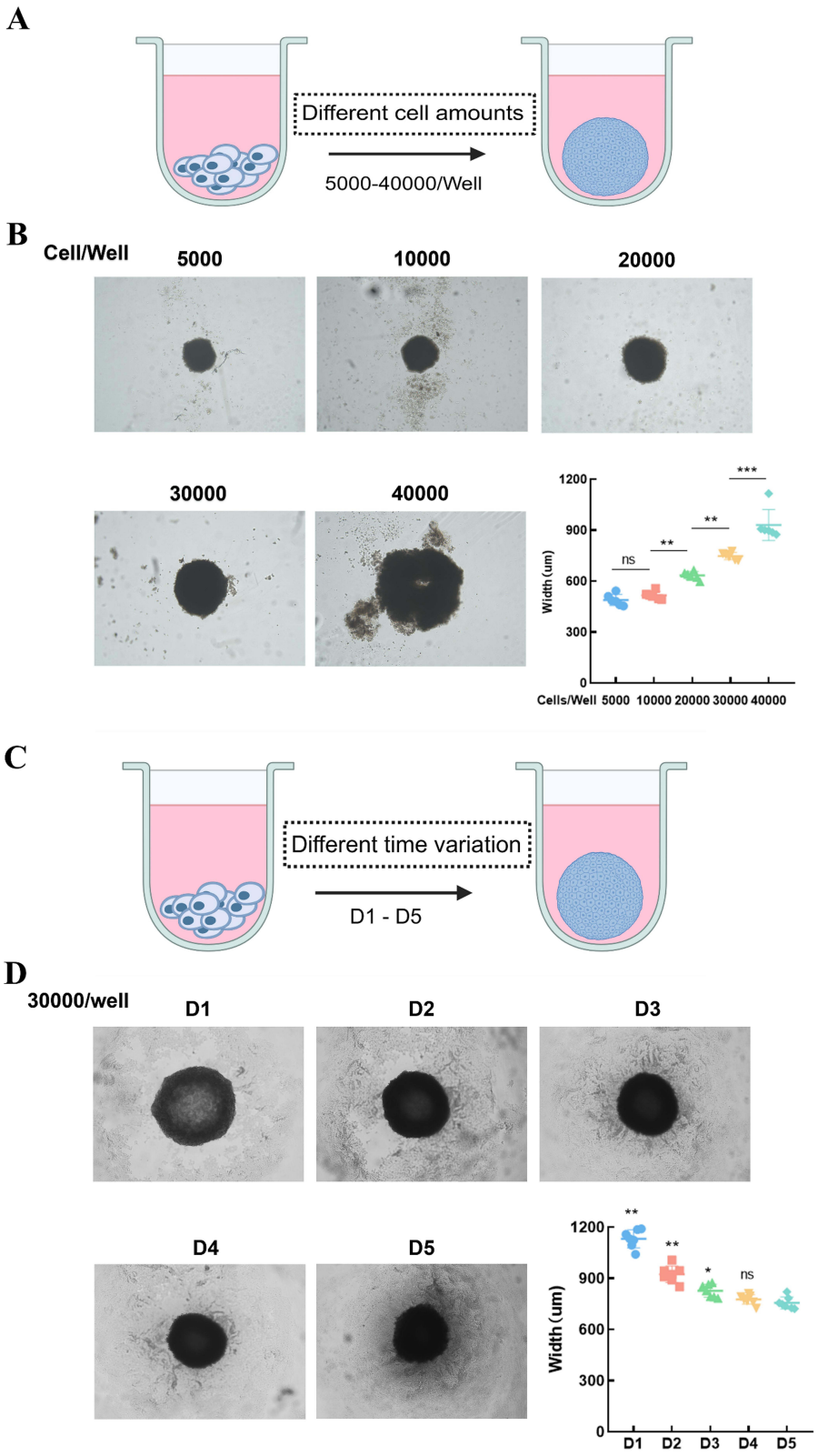

Figure 3 Optimal culture conditions for 3D chondrocytic spheroid. (**A**) Experimental Schematic: construction of 3D chondrocytic spheroids with varying cell amounts (5000–40000 cells/well). (**B**) Representative Images: 3D chondrocytic spheroids developed with different cell amounts, accompanied by a statistical analysis of spheroid diameters (n = 6). ***P*<0.01, ****P*<0.001, ns indicates no significant difference. (**C**) Experimental Schematic: construction of 3D chondrocytic spheroids at different time points (D1-D5). (**D**) Representative Images: 3D chondrocytic spheroids development from D1 to D5, along with a corresponding statistical analysis of spheroid diameters (n = 7). **P*<0.05, ***P*<0.01 *versus* D5, ns indicates no significant difference.

type II collagen (collagen II) in frozen sections of chondrocytic spheroids. The results revealed that collagen II was abundantly expressed within the chondrospheres (Figure 4), indicating that they effectively simulate the cartilage ECM.

Establishment of Synoviocytes-3D Chondrocytic Spheroids Coculture System and Evaluation

Synoviocytes-3D Chondrocytic Spheroids Coculture

SW-982 synoviocytes, with stable overexpression of eGFP, were co-cultured with the constructed 3D chondrocytic spheroids to assess the degree of invasion (Figure 5A). Initially, the distribution of synoviocytes within the co-culture system was observed. The results indicated that the newly introduced synoviocytes were evenly distributed throughout the culture system. Over time, these synoviocytes gradually settled to the bottom of the wells and made contact with the chondrospheres (Figure 5B). Flow cytometry analysis revealed that the invasion of $eGFP^+$ synoviocytes into the chondrocytic spheroids progressively increased with extended co-culture time (Figure 5C and D), along with a corresponding rise in the IR (Figure 5E).

Invasion Characteristics of Synoviocytes Into 3D Chondrocytic Spheroids Overexpressing ADAMTS5

To expand the scope of application of the 3D chondrocytic spheroids model established in this study, we constructed the model using the C28/I2 chondrocytes with stable expression of ADAMTS5, an enzyme that predominantly degrades AGG in the cartilage ECM. We evaluated the invasion characteristics of synoviocytes into these gene-edited chondrocytic spheroids. The results demonstrated a significant increase in synoviocytes invasion into spheroids overexpressing ADAMTS5 (Figure 6A). Analysis of the designed invasion indices indicated a significant decrease in the IDR of synoviocytes in ADAMTS5-overexpressing spheroids (Figure 6B and C), while both the IAR (Figure 6D) and IC (Figure 6E) were significantly increased. Additionally, flow cytometry results showed a marked increase in the invasion of synovial cells (Figure 6F and G) and the IR (Figure 6H) in

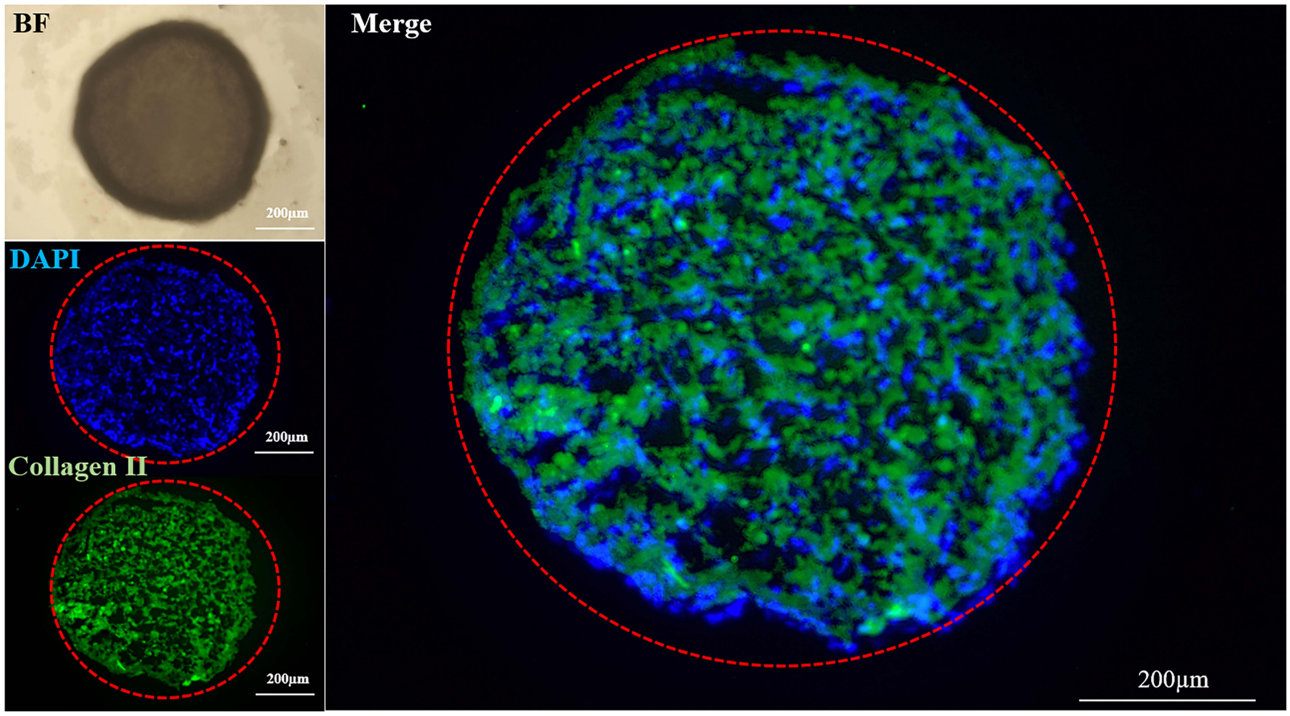

Figure 4 Detection of Collagen II expression in 3D chondrocytic spheroids. The expression of Collagen II in frozen section of 3D chondrocytic spheroids was measured by immunofluorescent staining. The red dotted circles show the outer outline of the 3D chondrocytic spheroids. Scale bar: 200 μm. BF: bright field.

https://doi.org/10.2147/JIR.S504701

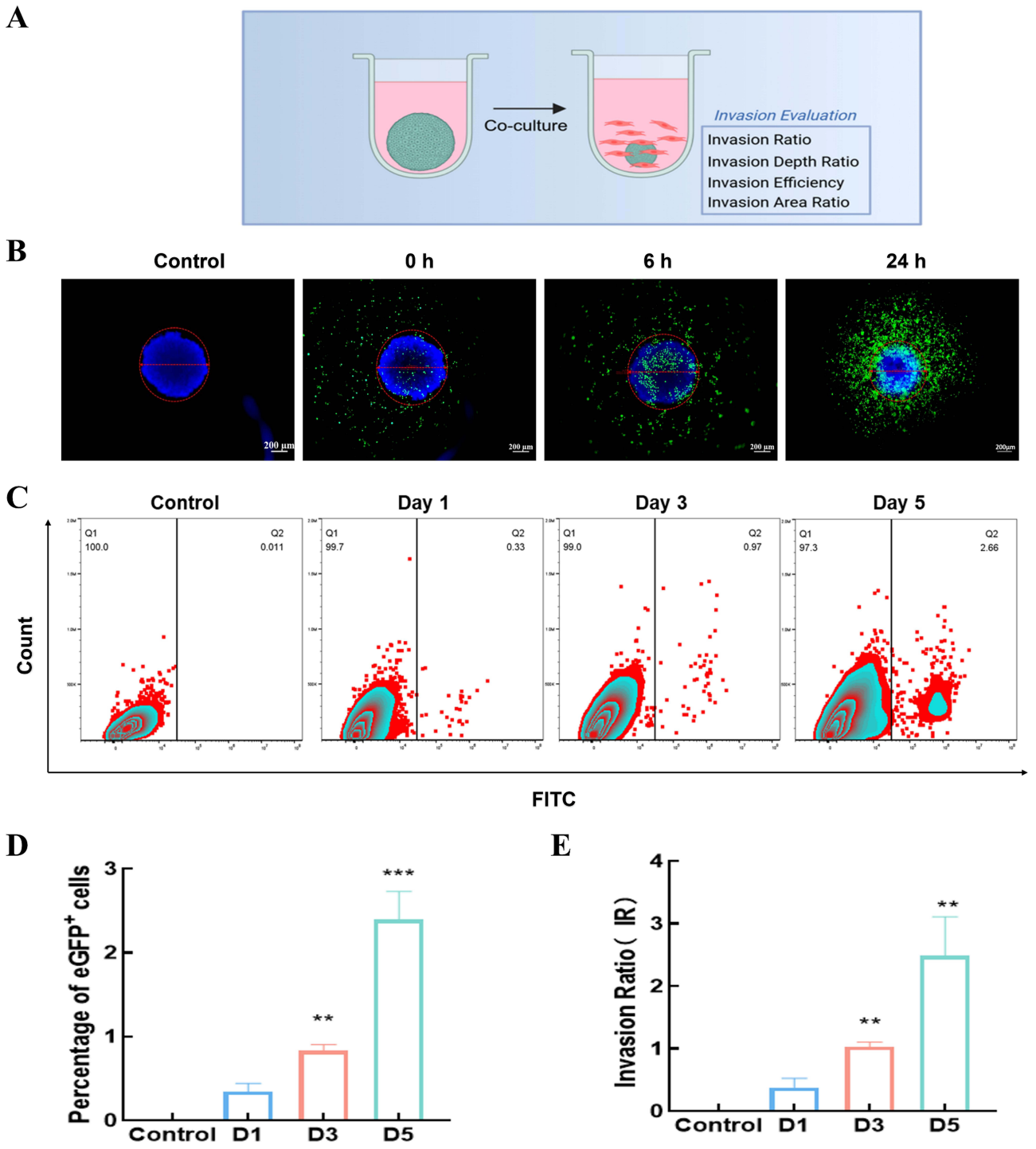

Figure 5 Observation of the invasion process of SW-982 synoviocytes into 3D chondrocytic spheroid in coculture system. (**A**) Experimental Schematic: an eGFP$^+$ SW-982 synoviocytes and 3D chondrocytic spheroid coculture system was established. Four indices, including Invasion Ratio, Invasion Depth Ratio, Invasion Count and Invasion Area Ratio were designed to estimate the invasion degree of synoviocytes. (**B**) Representative images of eGFP$^+$ SW-982 synoviocytes observed at different time points (0, 6 and 12 h) after being adding into the 3D chondrocytic spheroid coculture system. The 3D chondrocytic spheroids were stained with DAPI (blue), and SW-982 synoviocytes were transfected with eGFP (green). The red dotted circles show the outer outline of the 3D chondrocytic spheroids. Scale bar: 200 μm. (**C**) Flow cytometry was used to detect the invaded SW-982 synoviocytes, and analysis of (**D**) the percentage of eGFP$^+$ cells and (**E**) Invasion Ratio (n = 3). ***P*<0.01, ****P*<0.001 *versus* Control.

these ADAMTS5-overexpressing spheroids. These findings validate the 3D chondrosphere model constructed in this study as a suitable platform for gene-editing approaches and provide a novel methodology for investigating therapeutic targets pertinent to synoviocytes invasion into cartilage.

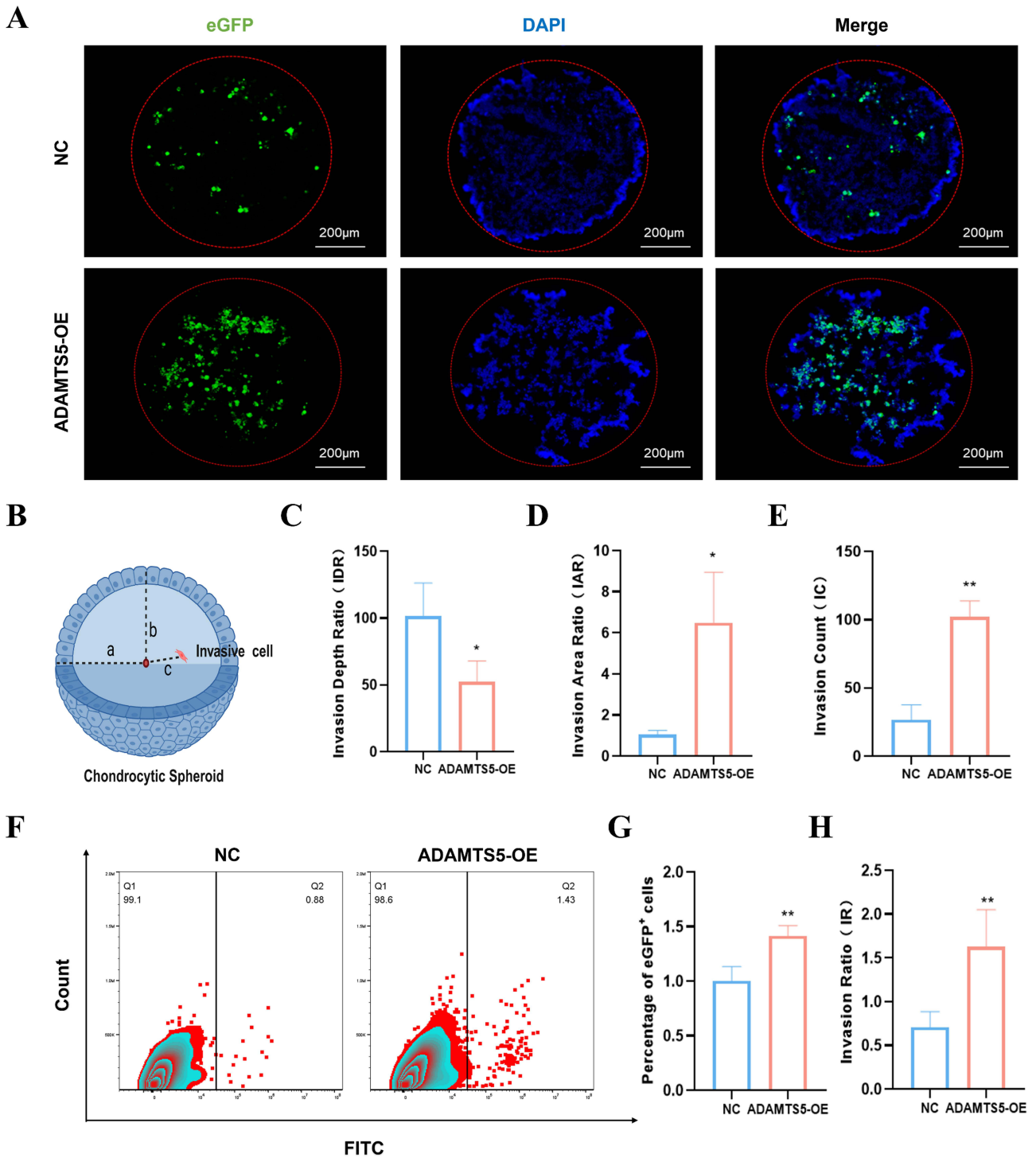

Figure 6 Evaluation of the invasive characteristics of SW-982 synoviocytes in 3D chondrocytic spheroids developed with ADAMTS5-overexpressing C28/I2 chondrocytes. (**A**) Representative images of invaded SW-982 synoviocytes (green) in 3D chondrocytic spheroids with ADAMTS5 overexpression. The red dotted circles show the outer outline of the 3D chondrocytic spheroids. Scale bar: 200 μm. (**B**) Schematic diagram shows the a, b and c for IDR analysis. Analysis of (**C**) IDR, (**D**) IAR and (**E**) IC to evaluate the invasion degree of SW-982 synoviocytes (n = 3). (**F**) Flow cytometry was used to detect the invaded SW-982 synoviocytes, and analysis of (**G**) the percentage of $eGFP^+$ cells and (**H**) Invasion Ratio (n = 3). **P*<0.05, ***P*<0.01 *versus* Negative Control (NC).

https://doi.org/10.2147/JIR.S504701

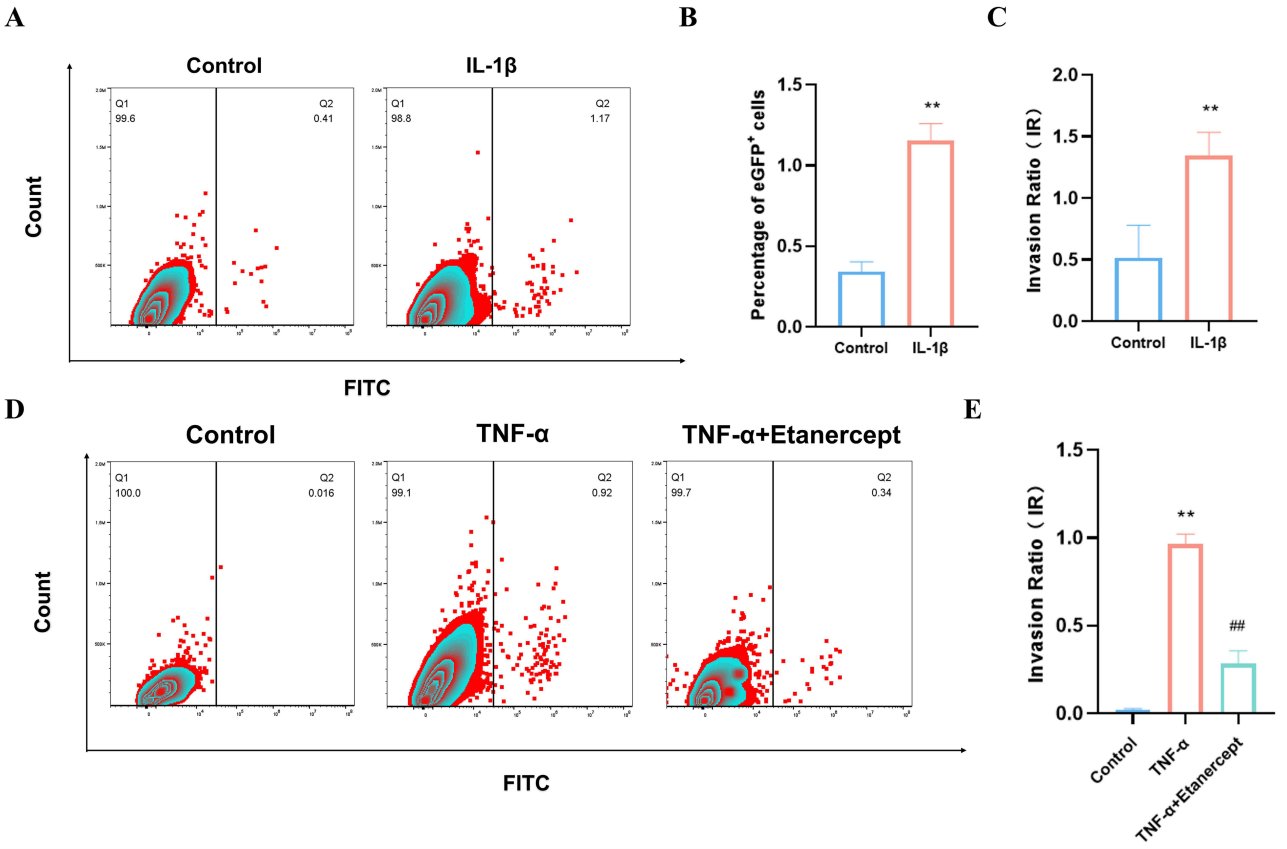

Figure 7 Evaluation of the invasive characteristics of SW-982 synoviocytes in 3D chondrocytic spheroids treated with inflammatory cytokines or drugs. (**A**) Flow cytometry was used to detect the invaded SW-982 synoviocytes in IL-1β treated 3D chondrocytic spheroids, and analysis of (**B**) the percentage of $eGFP^+$ cells and (**C**) Invasion Ratio (n = 3). (**D**) Flow cytometry was used to detect the invaded SW-982 synoviocytes in TNF-α and/or Etanercept (TNF-α inhibitor) treated 3D chondrocytic spheroids, and analysis of (**E**) the Invasion Ratio (n = 3). $^{**}P<0.01$ *versus* Control, $^{\#\#}P<0.01$ *versus* TNF-α.

Invasion Characteristics of Synoviocytes Into 3D Chondrocytic Spheroids Treated With Inflammatory Cytokines or Drugs

Inflammatory cytokines promote the invasion of synoviocytes by aberrantly activating chondrocytes, leading to the internal degradation of cartilage ECM. To further validate the utility of the 3D chondrocytic spheroids model in replicating synoviocytes invasion process, we pretreated the chondrocytic spheroids with inflammatory factors and subsequently examined the invasion characteristics of synoviocytes. Flow cytometry analysis revealed an increase in synoviocytes invasion (Figure 7A and B), as well as a corresponding rise in the IR (Figure 7C), following IL-1β treatment of the spheroids. Moreover, the abnormal activation of synovial cells driven by inflammatory factors is also a significant contributor to cartilage degradation. To investigate this phenomenon further, we pretreated SW-982 synoviocytes with TNF-α and/or its inhibitor Etanercept and assessed their invasion characteristics within the chondrocytic spheroids. As expected, TNF-α treatment enhanced the invasive capacity of SW-982 synoviocytes, while Etanercept successfully reversed this effect (Figure 7D and E).

Discussion

The drug discovery and development process are marked by its lengthy duration, complexity, and substantial financial costs, with the screening of novel therapeutic agents and their preclinical validation being critical bottlenecks. In vivo disease models are essential for validating the efficacy and toxicological profiles of therapeutic agents in the preclinical phase. However, due to ethical concerns, limited efficiency, and high costs, they are not suitable for high-throughput drug screening. Consequently, the development of appropriate in vitro disease models, along with their corresponding

evaluation systems, is crucial for advancing drug screening research and understanding the underlying biological mechanisms.

In pathological context, cell invasion generally refers to the process by which tumor cells traverse the basement membrane ECM through energy expenditure and the secretion of MMPs.[22] Interestingly, cell invasion is also observed in RA joints. In RA, synoviocytes, under the chronic influence of an inflammatory microenvironment, exhibit tumor-like pathological characteristics. They secrete significant amounts of MMPs, which degrade the cartilage ECM, thereby invading and contributing to tissue destruction.[2,4,23] Targeting this process offers a potential avenue for the development of novel therapeutic agents for RA. Currently, the accepted in vitro model for studying synoviocytes invasion uses matrigel to simulate cartilage ECM. However, matrigel's primary components—laminin, Col IV, and entactin—were initially designed to study tumor cell invasion and more closely resemble the basement membrane.[17,18] In contrast, cartilage ECM predominantly consists of Col II and AGG.[24] This discrepancy in composition could introduce bias into the drug screening process, underscoring the need for in vitro models that more accurately replicate cartilage ECM to facilitate the screening of novel therapeutics targeting synovial invasion of cartilage.

Traditional in vitro drug screening models, such as those used in anti-cancer drug screening, are typically based on 2D cell cultures where drug candidates are evaluated by their effects on cell proliferation and viability.[25] While effective, 2D cell cultures do not accurately replicate the physiological environment of cells, leading to limitations in the selectivity and sensitivity required for precise predictions of drug efficacy.[7,26] In light of these limitations, 3D cell culture systems are increasingly demonstrating their advantages in drug screening. These systems can include spheroids or organoids derived from a single cell line or organ-on-a-chip models differentiated from progenitor stem cells.[27,28] With advancements in 3D culture technology, there has been growing interest in 3D chondrocytes cultures. Researches have shown that chondrocytes cultured in 3D systems better maintain their inherent phenotype and ECM secretion characteristics.[15,29,30] In this study, we compared gene expression changes in C28/I2 chondrocytes cultured in 2D versus 3D environments using RNA-seq and PCR analysis. The results revealed that ECM synthesis-related pathways were significantly enriched in 3D cultured C28/I2 chondrocytes, while genes associated with inflammation, apoptosis, and matrix-degrading enzyme activity were markedly downregulated. These findings suggest that 3D culture systems more accurately simulate the natural growth environment of chondrocytes, helping to preserve their normal functions and laying a strong foundation for developing in vitro cartilage invasion models.

Cartilage is a critical component of synovial joints, providing cushioning and reducing friction within the joint.[23] It is primarily composed of chondrocytes and ECM. In RA, cartilage destruction is largely driven by the degradation of Col II and AGG in the ECM, caused by MMPs and ADAMTS enzymes secreted by synoviocytes and chondrocytes.[4,31,32] Therefore, accurately simulating cartilage ECM is essential for studying the pathological process of synovial invasion into cartilage. In this study, we developed a 3D chondrocytic spheroid model using a matrigel-free 3D culture technique. We optimized the conditions for establishing this model, including the number of cells seeded and the duration of culture. Additionally, we confirmed that the 3D chondrocytic spheroid model highly expresses Col II, the primary component of cartilage ECM. This indicates that the model effectively simulates the physiological state of cartilage and provides a robust foundation for evaluating the process of synovial invasion into cartilage.

The traditional transwell model for evaluating synovial invasion primarily relies on counting the number of synoviocytes that pass through the matrigel, offering a relatively simple assessment method.[33,34] In this study, building upon our established 3D chondrocytic spheroid model, we introduced several evaluation metrics, including IR, IDR, IAR, and IC, to more comprehensively assess the extent of synoviocytes invasion into cartilage. Furthermore, we tested the consistency and stability of this model using 3D chondrospheres overexpressing ADAMTS5, pretreated with IL-1β, and synovial cells treated with TNF-α, with or without Etanercept. The experimental results confirmed the model's feasibility for evaluating cartilage invasion by synoviocytes. This model thus provides an ideal platform for innovative drug screening and mechanistic research targeting the synovial invasion of cartilage.

Conclusion

In conclusion, the matrigel-free 3D chondrocytic spheroid model presented in this study provides significant advantages. It closely replicates the composition of cartilage, enables precise control over volume, and supports drug and gene

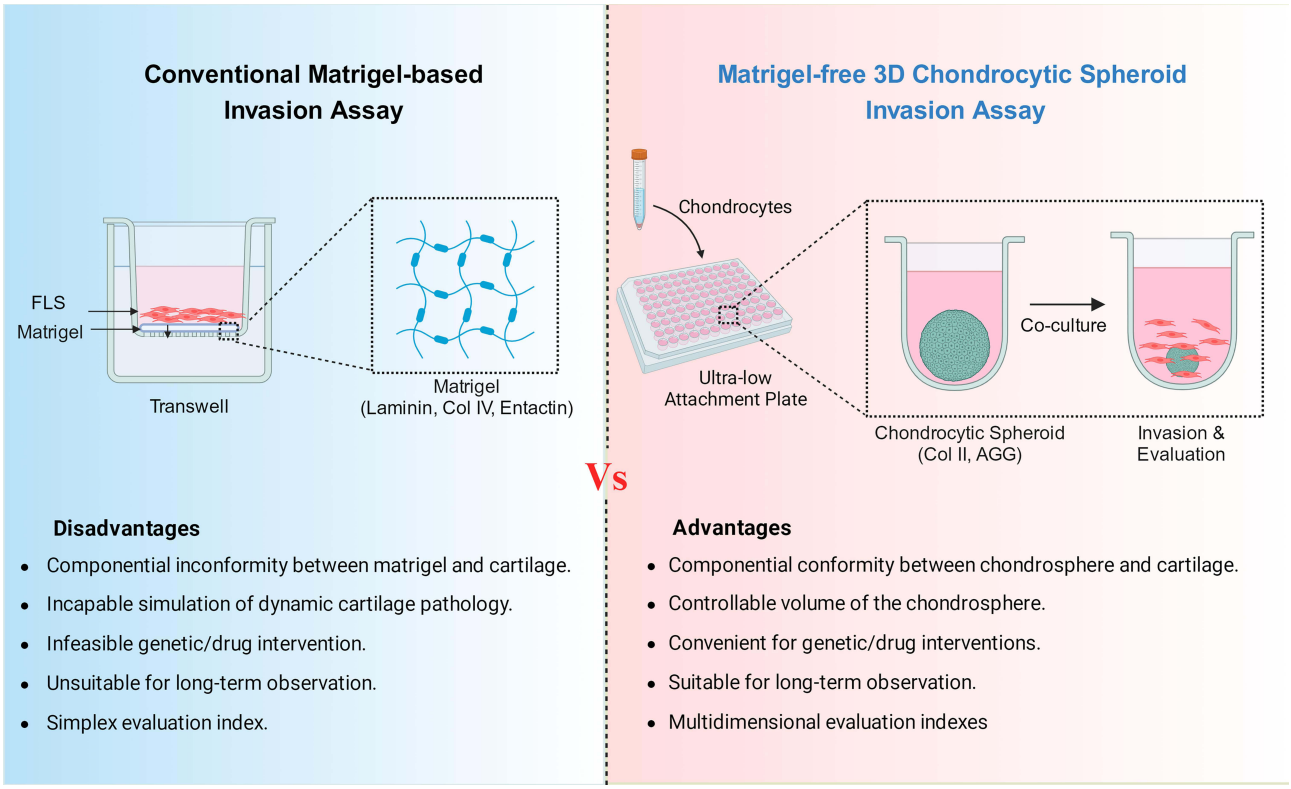

Figure 8 Schematic diagram of advantage for the matrigel-free 3D chondrocytic spheroid invasion model.

interventions. Its ability to accommodate long-term observation and multi-parameter evaluation makes it an ideal platform for drug screening and studying the pathogenesis of cartilage invasion by synoviocytes (Figure 8). The model's versatility suggests promising applications in various domains. For instance, by genetically modifying the chondrocytic spheroids based on patient-specific disease-associated genes, the model could be adapted to assess drug sensitivity in a personalized manner, facilitating tailored treatment strategies. Moreover, the model's flexibility may allow for its utilization in exploring other cartilage-related pathologies, such as osteoarthritis or cartilage regeneration, further expanding its clinical significance. However, while the model offers a more physiologically relevant environment and enhanced assessment capabilities, challenges related to scalability and its integration into high-throughput screening systems need to be addressed to optimize its utility further. These adjustments could help in advancing the model's application in routine drug discovery processes and personalized medicine, potentially accelerating the development of novel therapies for conditions like RA and other cartilage disorders.

Abbreviations

ADAMTS, A disintegrin and metalloproteinase with thrombospondin motifs; AGG, Aggrecan; Col, Collagen; ECM, Extracellular matrix; FLS, Fibroblast-like synoviocytes; IAR, Invasion area ratio; IC, Invasion counts; IDR, Invasion depth ratio; IL, Interleukin; IR, Invasion ratio; MMPs, Matrix metalloproteinases; RA, Rheumatoid arthritis; TNF, Tumor necrosis factor; 3D, Three-dimensional.

Data Sharing Statement

All data generated or analysed and materials used during this study are included in this article.

Consent for Publication

All authors consent to publication.

Funding

This study was supported by grants from the National Natural Science Foundation of China (No. 82204405, 82071591, 82304505), China Postdoctoral Science Foundation (No. 2024M750023, No. 2023M740026), Natural Science Foundation of Anhui Province (2408085MH217), National Funded Postdoctoral Researcher Program of China (GZC20230028), Young Elite Scientists Sponsorship Program by Anhui Association for Science and Technology (RCTJ202427), Overseas Visit and Study Program for Outstanding Young Talents in Colleges and Universities (gxgwfx2021011), National Natural Science Foundation Incubation Program of The Second Affiliated Hospital of Anhui Medical University (2021GQFY01, 2021GMFY06).

Disclosure

The authors declare they have no competing interests in this work.

References

1. Gravallese EM, Firestein GS. Rheumatoid arthritis - common origins, divergent mechanisms. *N Engl J Med*. 2023;388(6):529–542. doi:10.1056/NEJMra2103726
2. Yang X, Zhao Y, Wei Q, et al. GRK2 inhibits Flt-1(+) macrophage infiltration and its proangiogenic properties in rheumatoid arthritis. *Acta Pharm Sin B*. 2024;14(1):241–255. doi:10.1016/j.apsb.2023.09.013
3. Mankia K, Di Matteo A, Emery P. Prevention and cure: the major unmet needs in the management of rheumatoid arthritis. *J Autoimmun*. 2020;110:102399. doi:10.1016/j.jaut.2019.102399
4. Nygaard G, Firestein GS. Restoring synovial homeostasis in rheumatoid arthritis by targeting fibroblast-like synoviocytes. *Nat Rev Rheumatol*. 2020;16(6):316–333. doi:10.1038/s41584-020-0413-5
5. Yao F, Zhao Y, Yu Q, et al. Extracellular CIRP induces abnormal activation of fibroblast-like synoviocytes from patients with RA via the TLR4-mediated HDAC3 pathways. *Int Immunopharmacol*. 2024;128:111525. doi:10.1016/j.intimp.2024.111525
6. Katoh S, Yoshioka H, Senthilkumar R, Preethy S, Abraham SJK. Enhanced miRNA-140 expression of osteoarthritis-affected human chondrocytes cultured in a polymer based three-dimensional (3D) matrix. *Life Sci*. 2021;278:119553. doi:10.1016/j.lfs.2021.119553
7. Wang Y, Jeon H. 3D cell cultures toward quantitative high-throughput drug screening. *Trends Pharmacol Sci*. 2022;43(7):569–581. doi:10.1016/j.tips.2022.03.014
8. Raveendran N, Vaswani K, Han P, Basu S, Moran CS, Ivanovski S. Modeling inflammatory response using 3D bioprinting of polarized macrophages. *Int J Bioprinting*. 2024;10(2):398–412. doi:10.36922/ijb.2116
9. Xu Y, Pachnikova G, Wang H, et al. IC50: an unsuitable measure for large-sized prostate cancer spheroids in drug sensitivity evaluation. *Bosn J Basic Med Sci*. 2022;22(4):580–592. doi:10.17305/bjbms.2022.7279
10. Vila-Parrondo C, Garcia-Astrain C, Liz-Marzan LM. Colloidal systems toward 3D cell culture scaffolds. *Adv Colloid Interface Sci*. 2020;283:102237. doi:10.1016/j.cis.2020.102237
11. Hipwood L, Clegg J, Weekes A, et al. Semi-synthetic click-gelatin hydrogels as tunable platforms for 3D cancer cell culture. *Gels*. 2022;8(12):821. doi:10.3390/gels8120821
12. Kaur S, Kaur I, Rawal P, Tripathi DM, Vasudevan A. Non-matrigel scaffolds for organoid cultures. *Cancer Lett*. 2021;504:58–66. doi:10.1016/j.canlet.2021.01.025
13. Khajehmohammadi M, Bakhtiary N, Davari N, et al. Bioprinting of cell-laden protein-based hydrogels: from cartilage to bone tissue engineering. *Int J Bioprinting*. 2023;9(6):466–501. doi:10.36922/ijb.1089
14. Rosenzweig DH, Carelli E, Steffen T, Jarzem P, Haglund L. 3D-printed ABS and PLA scaffolds for cartilage and nucleus pulposus tissue regeneration. *Int J mol Sci*. 2015;16(7):15118–15135. doi:10.3390/ijms160715118
15. Lindberg ED, Wu T, Cotner KL, et al. Priming chondrocytes during expansion alters cell behavior and improves matrix production in 3D culture. *Osteoarthritis Cartilage*. 2024;32(5):548–560. doi:10.1016/j.joca.2023.12.006
16. Kuang Y, Li R, Wang J, et al. ALKBH5-mediated RNA m(6) A methylation regulates the migration, invasion, and proliferation of rheumatoid fibroblast-like synoviocytes. *Arthritis Rheumatol*. 2024;76(2):192–205. doi:10.1002/art.42676
17. Benton G, Arnaoutova I, George J, Kleinman HK, Koblinski J. Matrigel: from discovery and ECM mimicry to assays and models for cancer research. *Adv Drug Deliv Rev*. 2014;79-80:3–18. doi:10.1016/j.addr.2014.06.005
18. Albini A. Extracellular matrix invasion in metastases and angiogenesis: commentary on the matrigel "chemoinvasion assay". *Cancer Res*. 2016;76(16):4595–4597. doi:10.1158/0008-5472.CAN-16-1971
19. Ouyang Z, Dong L, Yao F, et al. Cartilage-related collagens in osteoarthritis and rheumatoid arthritis: from pathogenesis to therapeutics. *Int J mol Sci*. 2023;24(12):9841. doi:10.3390/ijms24129841
20. Jacobs CA, Keller LE, Zhang S, et al. Periostin regulation and cartilage degradation early after anterior cruciate ligament reconstruction. *Inflamm Res*. 2023;72(3):387–394. doi:10.1007/s00011-022-01678-9
21. Zhao Y, Yang X, Li S, et al. sTNFRII-Fc modification protects human UC-MSCs against apoptosis/autophagy induced by TNF-alpha and enhances their efficacy in alleviating inflammatory arthritis. *Stem Cell Res Ther*. 2021;12(1):535. doi:10.1186/s13287-021-02602-4
22. Garde A, Sherwood DR. Fueling cell invasion through extracellular matrix. *Trends Cell Biol*. 2021;31(6):445–456. doi:10.1016/j.tcb.2021.01.006
23. Zhou R, Chen Y, Li S, et al. TRPM7 channel inhibition attenuates rheumatoid arthritis articular chondrocyte ferroptosis by suppression of the PKCalpha-NOX4 axis. *Redox Biol*. 2022;55:102411. doi:10.1016/j.redox.2022.102411
24. Zhou RP, Chen Y, Wei X, et al. Novel insights into ferroptosis: implications for age-related diseases. *Theranostics*. 2020;10(26):11976–11997. doi:10.7150/thno.50663

25. Chan YT, Lu Y, Wu J, et al. CRISPR-Cas9 library screening approach for anti-cancer drug discovery: overview and perspectives. *Theranostics*. 2022;12(7):3329–3344. doi:10.7150/thno.71144
26. Pound P, Ritskes-Hoitinga M. Is it possible to overcome issues of external validity in preclinical animal research? Why most animal models are bound to fail. *J Transl Med*. 2018;16(1):304. doi:10.1186/s12967-018-1678-1
27. Grimes DR, Currell FJ. Oxygen diffusion in ellipsoidal tumour spheroids. *J R Soc Interface*. 2018;15(145):20180256. doi:10.1098/rsif.2018.0256
28. Schuster B, Junkin M, Kashaf SS, et al. Automated microfluidic platform for dynamic and combinatorial drug screening of tumor organoids. *Nat Commun*. 2020;11(1):5271. doi:10.1038/s41467-020-19058-4
29. Ding SL, Zhao XY, Xiong W, et al. Cartilage lacuna-inspired microcarriers drive hyaline neocartilage regeneration. *Adv Mater*. 2023;35(30):e2212114. doi:10.1002/adma.202212114
30. Shim HE, Kim YJ, Park KH, Park H, Huh KM, Kang SW. Enhancing cartilage regeneration through spheroid culture and hyaluronic acid microparticles: a promising approach for tissue engineering. *Carbohydr Polym*. 2024;328:121734. doi:10.1016/j.carbpol.2023.121734
31. Liu D, Li R, Xu S, et al. SMOC2 promotes aggressive behavior of fibroblast-like synoviocytes in rheumatoid arthritis through transcriptional and post-transcriptional regulating MYO1C. *Cell Death Dis*. 2022;13(12):1035. doi:10.1038/s41419-022-05479-0
32. Yang X, Zhang W, Wang L, Zhao Y, Wei W. Metabolite-sensing GPCRs in rheumatoid arthritis. *Trends Pharmacol Sci*. 2024;45(2):118–133. doi:10.1016/j.tips.2023.12.001
33. Symons RA, Colella F, Collins FL, et al. Targeting the IL-6-Yap-snail signalling axis in synovial fibroblasts ameliorates inflammatory arthritis. *Ann Rheum Dis*. 2022;81(2):214–224. doi:10.1136/annrheumdis-2021-220875
34. Lin X, Lin T, Wang X, et al. Sesamol serves as a p53 stabilizer to relieve rheumatoid arthritis progression and inhibits the growth of synovial organoids. *Phytomedicine*. 2023;121:155109. doi:10.1016/j.phymed.2023.155109